Molecular Therapy
Methods & Clinical Development
Original Article

Low incidence of hepatocellular carcinoma in mice and cats treated with systemic adeno-associated viral vectors

Rita Ferla,[1,2] Marialuisa Alliegro,[1,2] Margherita Dell'Anno,[1,2] Edoardo Nusco,[1] John M. Cullen,[3] Stephanie N. Smith,[4] Tyra G. Wolfsberg,[4] Patricia O'Donnell,[5] Ping Wang,[5] Anh-Dao Nguyen,[4] Randy J. Chandler,[4] Zelin Chen,[4] Shawn M. Burgess,[4] Charles H. Vite,[5] Mark E. Haskins,[5] Charles P. Venditti,[4] and Alberto Auricchio[1,6]

[1]Telethon Institute of Genetics and Medicine (TIGEM), 80078 Pozzuoli, Naples, Italy; [2]Medical Genetics, Department of Translational Medicine, "Federico II" University, 80131 Naples, Italy; [3]North Carolina College of Veterinary Medicine, Raleigh, NC 27607, USA; [4]National Human Genome Research Institute, NIH, Bethesda, MD 20892, USA; [5]Department of Pathobiology, School of Veterinary Medicine, University of Pennsylvania, Philadelphia, PA 19104, USA; [6]Medical Genetics, Department of Advanced Biomedicine, "Federico II" University, 80131 Naples, Italy

Adeno-associated viral (AAV) vectors have emerged as the preferred platform for *in vivo* gene transfer because of their combined efficacy and safety. However, insertional mutagenesis with the subsequent development of hepatocellular carcinomas (HCCs) has been recurrently noted in newborn mice treated with high doses of AAV, and more recently, the association of wild-type AAV integrations in a subset of human HCCs has been documented. Here, we address, in a comprehensive, prospective study, the long-term risk of tumorigenicity in young adult mice following delivery of single-stranded AAVs targeting liver. HCC incidence in mice treated with therapeutic and reporter AAVs was low, in contrast to what has been previously documented in mice treated as newborns with higher doses of AAV. Specifically, HCCs developed in 6 out 76 of AAV-treated mice, and a pathogenic integration of AAV was found in only one tumor. Also, no evidence of liver tumorigenesis was found in juvenile AAV-treated mucopolysaccharidosis type VI (MPS VI) cats followed as long as 8 years after vector administration. Together, our results support the low risk of tumorigenesis associated with AAV-mediated gene transfer targeting juvenile/young adult livers, although constant monitoring of subjects enrolled in AAV clinical trial is advisable.

INTRODUCTION

Adeno-associated viral (AAV) vectors are the most used viral vectors for *in vivo* gene transfer because of both their ability to ensure long-term transduction of a wide spectrum of tissues and their safety profile.[1] Indeed, wild-type AAVs, from which AAV vectors derive, do not exhibit pathogenicity in humans as their lytic stage occurs only in the presence of a helper virus.[2] In recombinant AAV vectors, viral sequences involved in replication, site-specific genome integration, and capsid production are replaced by a transgene expression cassette, which is flanked by the inverted terminal repeats (ITRs) that are necessary for DNA packaging. This makes conventional recombinant AAV vectors replication-defective, and, without a source of Rep, unable to integrate into *AAVS1* or similar sites. Thus, recombinant AAVs (rAAVs) largely persist as episomes in the nucleus of transduced cells, which minimizes the risk of related genotoxicity. However, integration of recombinant AAV is well recognized and has been reported to occur with a low frequency and a preference for loci close to active genes or CpG islands.[3,4]

The universally accepted safety of AAV vectors has been recently questioned by several studies documenting insertional mutagenesis and hepatocellular carcinoma (HCC) formation following liver gene transfer in newborn mice.[5–7] In HCCs, AAV was found integrated into the RNA imprinted and accumulated in nucleus (*Rian*) locus,[5,6] which encodes for many regulatory non-coding RNAs, leading to deregulation of genes flanking the insertion site and promoting HCC development.[5] Consistent with the importance of the *Rian* locus in hepatic biology, the overexpression of the human orthologs within the *Rian* locus, such as the delta-like homolog 1-deiodinase type 3 (*DLK1-DIO3*) gene, has been associated with poor survival in humans with hepatic carcinoma.[8] However, the majority of AAV integrations into the *Rian* locus were located in *Mir341*, which does not have an ortholog in humans.[5] Interestingly, Chandler et al.[5] demonstrated that HCC development strongly correlates with AAV dosing and was influenced by the enhancer/promoter used; in particular, the chicken beta actin (CBA) and the thyroxine-binding globulin (TBG) promoters, but not the liver-specific promoter 1 (LP1), were able to induce the gene deregulation responsible for HCC development in mice. Also, genes known to have a high expression in the

Received 2 September 2020; accepted 19 November 2020;
https://doi.org/10.1016/j.omtm.2020.11.015.

Correspondence: Rita Ferla, PhD, Telethon Institute of Genetics and Medicine (TIGEM), Via Campi Flegrei 34, Pozzuoli 80078, Italy.
E-mail: ferla@tigem.it
Correspondence: Alberto Auricchio, MD, Telethon Institute of Genetics and Medicine (TIGEM), Pozzuoli 80078, Italy.
E-mail: auricchio@tigem.it

Table 1. Experimental groups

Groups	Number of animals	Treatment	Dose (GC/kg)
CTR 1	10M + 10F	None	N/A
CTR 2	10M + 10F	Excipient 1	N/A
CTR 3	5M + 5F	Excipient 2	N/A
TEST 1	10M + 10F	AAV2/8.TBG.*hARSB*	2×10^{13}
TEST 2	10M + 10F	AAV2/8.TBG.*hARSB*	2×10^{12}
TEST 3	10M + 10F	AAV2/8.LP1.*hARSB*	2×10^{13}
TEST 4	10M + 10F	AAV2/8.TBG.*EGFP*	2×10^{13}

CTR, control group; TEST, test group; M, male; F, female; Excipient 1, PBS/5% glycerol diluted 1:1.5 in saline solution NaCl 0.9%, as representative of formulation of vectors used in TEST 1, 3, and 4 groups; Excipient 2, PBS/5% glycerol diluted 1:15 in saline solution NaCl 0.9%, as representative of vector formulation used in TEST 2 group; GC, genome copies; N/A, not applicable.

neonatal liver, such as albumin (*Alb*), alpha-fetoprotein (*Afp*), and the *Rian* locus, were the most susceptible to AAV integration.[5,6] This suggests that the different liver gene-expression pattern of neonatal mice compared to juvenile and adult mice may affect AAV vector integration, and thus may limit the relevance of AAV-HCC observations to neonatal liver gene transfer. In line with this, insertional mutagenesis leading to HCC formation has not been reported following AAV administration to juvenile or adult mice,[9–11] and, importantly, *Rian* integrations were not found,[11,12] indicating that the locus is likely not accessible at later stages of life, presumably because the expression of *Rian* encoded genes is low in juvenile/adults compared to newborn mice.[7] The only exception reported is in adult AAV-treated ornithine transcarbamylase (OTC)-deficient mice, which however have a high background of spontaneous liver nodules and HCC formation.[13]

Because HCC formation after AAV gene therapy has been documented in a number of preclinical studies, we have performed an *ad hoc* study to evaluate the potential risk of tumorigenesis associated with AAV liver gene transfer in joung adult mice. More specifically, we sought to examine the vector used in a gene therapy clinical trial for mucopolysaccharidosis type VI (MPS VI), which is based on a single systemic administration of an AAV vector serotype 8 (AAV2/8) encoding the therapeutic transgene product, i.e., the human arylsulfatase B (*hARSB*), under the control of the TBG promoter (AAV2/8.TBG.*hARSB*, NTC03173521).

The MPS VI clinical trial population is targeting patients over the age of 4 years, a time point that was selected to minimize hepatic dilution of AAV genomes caused by liver growth during the first years of life. The age criteria were also informed by our studies with newborn MPS VI cats,[14] where a reduction of ARSB levels followed vector administration. Therefore, in the current study, we treated joung adult (6–8 week old) mice, in which hepatocyte proliferation is reduced compared to newborn mice, thus mimicking subjects that will be enrolled in the trial, with variable doses of AAV, and followed them long term to document HCC formation compared to controls.

In parallel, the long-term safety of AAV2/8.TBG.*ARSB* was assessed in MPS VI cats dosed at post-natal day 50 with 2×10^{12} genome copies (GC)/kg, a dose that was subsequently used the clinical trial.

RESULTS

Incidence of HCC and other tumors following AAV-mediated liver gene transfer in young adult mice

Young adult C57BL/6 mice received a single intravenous administration of AAV2/8 vectors encoding the *hARSB* under the control of either the TBG (AAV2/8.TBG.*hARSB*, either 2×10^{13} or 2×10^{12} GC/kg), or the LP1 promoter, (AAV2/8.LP1.*hARSB* [2×10^{13} GC/kg]) or encoding the enhanced green fluorescent protein (*EGFP*) under the control of TBG promoter (AAV2/8.TBG.*EGFP* [2×10^{13} GC/kg]). The control mice received the excipient alone or were left untreated (Table 1). Mice were followed-up to 24 months post-injection, i.e., about 26 months of age, unless euthanasia was required because of poor health conditions as revealed by clinical observations, i.e., abdominal palpation and cage-side evaluation. Histopathology was performed on all livers and any other organs showing gross abnormalities at necropsy (Figure S1).

Tumors were classified as HCC based on standard criteria (International Harmonization of Nomenclature and Diagnostic Criteria, INHAND) including pleomorphism, abnormal trabecular formation, and local invasion into the adjacent parenchyma. Representative pictures of proliferative hepatocellular lesions compared to normal liver are shown in Figures 1A and 1B.

HCCs were not found in control mice (0 out of 46; 24 males and 22 females), while in mice receiving AAV2/8 vectors, HCCs were reported only in males (6 out of 39) with an overall incidence of 15.4% ($p = 0.07$) but not in females (0 out 37).

Specifically, HCCs were found in 1 out of 10 (10%) male mice receiving 2×10^{13} GC/kg and 1 (which had both a hepatocellular adenoma [HCA] and an HCC) out 9 (11%) male mice receiving 2×10^{12} GC/kg of AAV2/8.TBG.*hARSB* (Figure 1C). No statistically significant differences were found between the two different dose cohorts ($p = 1$) and between each one of the cohorts and the controls ($p = 0.3448$ and 0.3913 for the dose of 2×10^{13} GC/kg and 2×10^{12} GC/kg, respectively), which suggests that the AAV dose in the ranges we tested did not affect HCC development in young adult AAV-treated C57BL/6 mice.

In the cohort of male mice receiving 2×10^{13} GC/Kg of AAV, HCCs incidence was similar (1 out 10, 10%) between mice receiving AAV2/8.TBG. and LP1.*hARSB* ($p = 1$; Figure 1C).

Overall, HCC incidence in male mice receiving AAV2/8.*hARSB* vectors was close to the reported spontaneous HCC formation rate; that is, 8%–9% in C57BL/6 male mice aged 22–27 months and not significantly different than in control groups ($p = 0.2425$).[9,15]

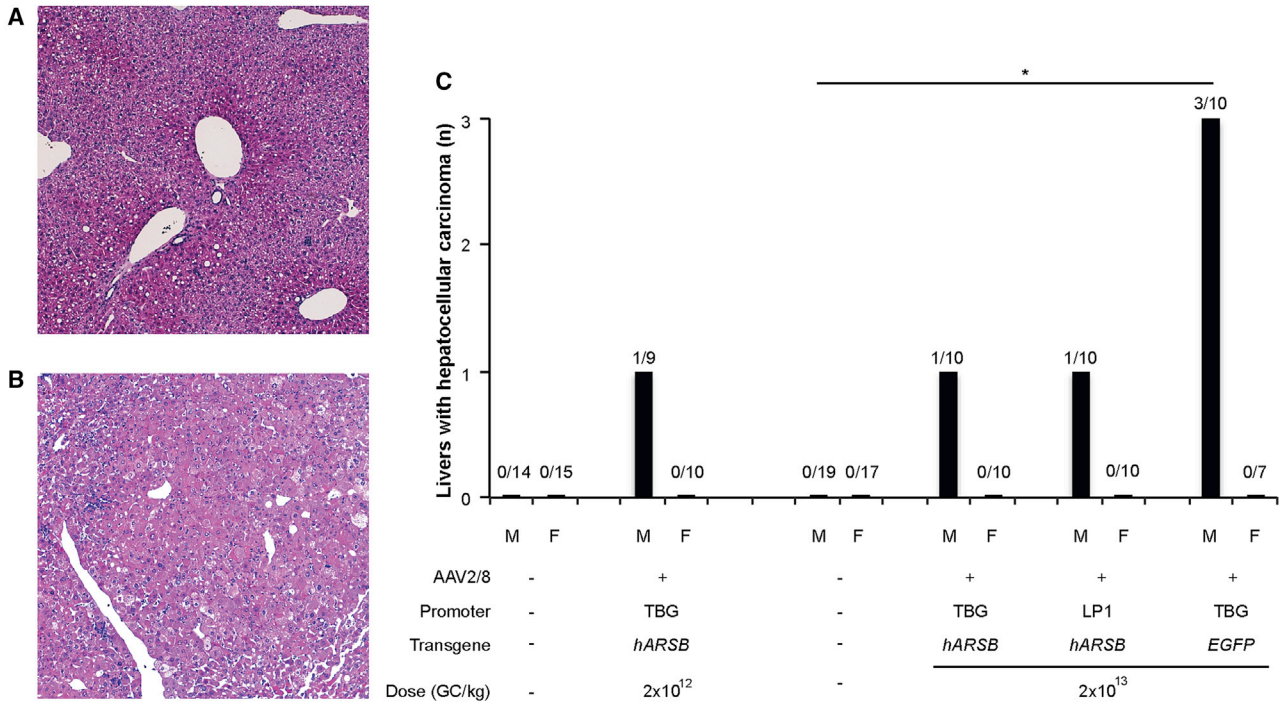

Figure 1. HCCs in young adult mice receiving AAV-mediated liver gene transfer

Histopathology was performed by H&E staining on all available livers from controls and AAV-treated mice. (A and B) Representative pictures of a normal liver (A) and a liver with HCC (B) are shown. Magnification is 50X. The graph (C) reports the number of livers with HCC found in male and female mice receiving AAV2/8 vectors and in control mice. Controls are: (1) mice left untreated and treated with the excipient 2 for mice receiving AAV at the dose 2×10^{12} GC/kg and (2) mice left untreated and treated with the excipient 1 for mice administered with AAV at the dose of 2×10^{13} GC/kg. The number of livers with HCC out of the number of total livers analyzed by histopathology is reported above each bar. Statistical comparisons were made using the Fisher test. The p value versus sex-matched controls is: *p < 0.05. AAV2/8, adeno-associated viral vectors serotype 8; TBG, thyroxine-binding globulin; LP1, liver-specific promoter 1; *hARSB*, human arylsulfatase B; *EGFP*, enhanced green fluorescence protein; M, male; F, female.

Conversely, HCCs were reported in 3 out of 10 male mice that received 2×10^{13} GC/kg of AAV2/8.TBG.*EGFP*. Unlike the other experimental groups, the HCC incidence (30%) was significantly different compared to controls (p = 0.03; Figure 1C). The HCC incidence was higher, albeit not significantly (p = 0.582), than in male mice receiving the same dose of AAV2/8.TBG.*hARSB* (10%). Notably, 2 out of 10 male mice injected with 2×10^{13} GC/kg of AAV2/8.TBG.*EGFP* developed hepatocellular adenomas, which increased the overall incidence of hepatic neoplasms in this experimental group to 50% (p versus control = 0.002, p versus AAV2/8.TBG.*hARSB* = 0.3498).

Other tumors found in livers, as well as in other organs such as the intestine, pancreas, spleen, neck, and ovary, were classified as round cell neoplasms, which include lymphoma, histiocyte-associated lymphoma, or histiocytic sarcomas as possible cell types. No additional characterization of these tumors was performed. No increase in the incidence of these round cells neoplasms was found in AAV-injected groups compared to controls (29% versus 22%, respectively; p = 0.40), as these tumors are reported to spontaneously arise in C57BL/6 mice as they age.[16] One hemangiosarcoma, one fibrosarcoma, and one stellate cell tumor were also found.

Elevated serum alpha-fetoprotein (AFP) has been reported associated with both human and murine HCC; moreover, AFP has been reported to remain below the threshold of 100 ng/mL in mice without hepatic tumors.[17,18] Accordingly, we found that serum AFP progressively increased over time in mice bearing either HCA and/or HCC, while it remained unchanged in mice without tumors (Figure S2). Specifically, we found that serum AFP levels above 100 ng/mL strongly correlated with HCC (p = 6.48e-10).

Similarly to what was observed in mice without tumors, we found no increase in AFP in mice bearing other solid tumors including round cell neoplasms found in livers, confirming these are not primary hepatic tumors and further supporting the concept that AFP can be considered as a marker of hepatocellular tumorigenesis in mice.

We also measured AAV GC in liver and serum ARSB activity in AAV-treated male and female mice. As expected, both GC and serum ARSB activity were significantly lower in mice receiving 2×10^{12} GC/kg than in mice receiving 2×10^{13} GC/kg (Figures 2A and 2B). In mice receiving 2×10^{12} GC/kg of AAV2/8.TBG.*hARSB*, males showed about 7-fold higher levels of GC per molecule of diploid genome (mdg) than females (0.13 ± 0.03 versus 0.02 ± 0.03 GC/mdg,

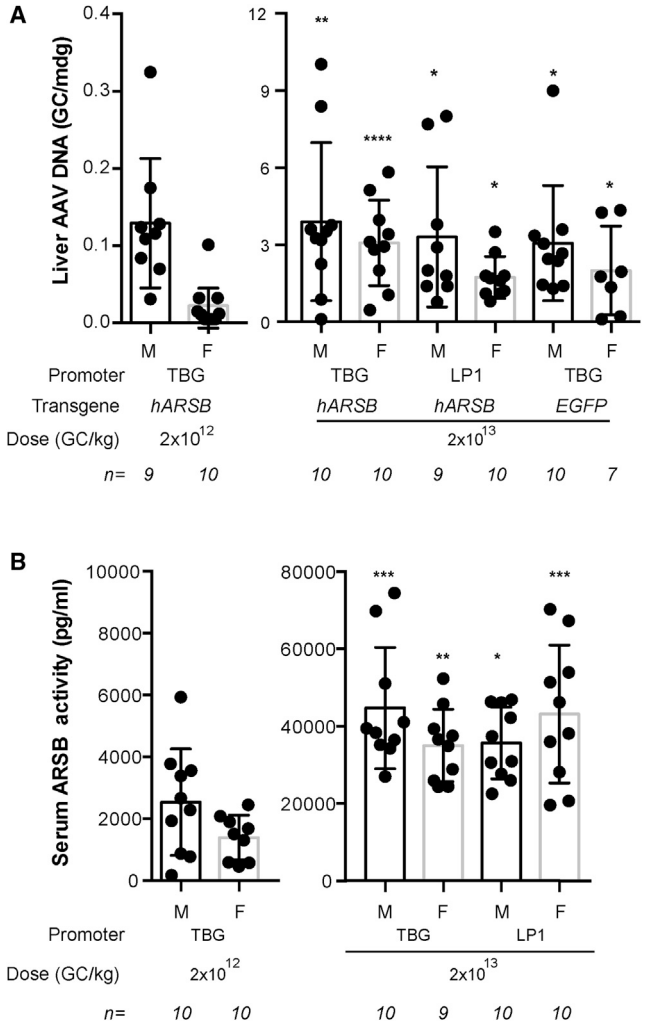

Figure 2. AAV liver DNA and serum ARSB activity in AAV-treated male and female mice

(A) AAV DNA was measured in liver of C57BL/6 males and females treated with AAV vectors. Results are expressed as GC/molecule of diploid genome (mdg). (B) Serum ARSB activity was measured in C57BL/6 males and females 1 year after the injection of AAV2/8 vectors encoding *hARSB*. Results are presented in (A) and (B) as mean measurement for each mouse (dot) and mean ± SE for each group of treatment (column). The number of mice analyzed is reported in the graph, below each column. Statistical comparisons were made using the Kruskal-Wallis test followed by Dunn's test; the p value versus sex-matched mice treated with 2×10^{12} GC/kg are *p < 0.05; **p < 0.01; ***p < 0.001; ****p < 0.0001. AAV2/8, adeno-associated viral vectors serotype 8; TBG, thyroxine-binding globulin; LP1: liver-specific promoter 1; *hARSB*, human arylsulfatase B; *EGFP*, enhanced green fluorescent protein; GC, genome copies; M, male; F, female.

respectively, Figure 2A). This difference was not statistically significant when the Kruskal-Wallis test followed by the Dunn's test was applied for multiple pairwise comparisons and became significant (p = 0.0012) when direct comparison between males and females was performed by Wilcoxon rank sum test. As shown in Figure 2B, serum ARSB activity was higher, albeit not significantly, in males than in females (2,531 ± 544 versus 1,391 ± 256 pg/mL, respectively; p = 0.09; Wilcoxon test). Conversely, no gender-related differences were observed in mice treated with 2×10^{13} GC/kg of AAV2/8 vectors in terms of either liver AAV GC or serum ARSB activity.

Integration analysis

We extracted genomic DNA from mouse HCCs, as well as from healthy surrounding tissue, where available, prepared libraries that were then barcoded, amplified, and subjected to high throughput sequencing using the Illumina MiSeq platform. The grouped reads were aligned to the mouse genome using the Genomic Integration Site Tracker pipeline (https://github.com/mlafave/GeIST) with an additional step that discarded all reads that mapped to the vectors.[5,19] Furthermore, in an effort to remove any possible protocol-induced artifacts, we also removed integration sites (ISs) that were seen in any other mouse AAV integration study previously performed using this pipeline (Wolfsberg et al., unpublished data).[5]

We analyzed data from 6 animals. For three of the mice (81, 85, and 99), we studied both HCC and control samples, and we analyzed the HCC and control data separately. For another three mice (51, 94, and 95) we had only HCC samples, and we pooled these data together with the HCC data from the first three mice, using the pool of all control samples for comparison. The first step was to identify the number of ISs for each group. We report both the total number of ISs in each group, as well as the number of unique ISs if each genomic position is counted only once (Table S1).

Based on previous work,[5] we only pursued integrations that were present in HCCs but not in controls and had high read counts, suggesting clonality. Only one integration site with a strikingly high read count (>40,000 reads) emerged after filtering based on read counts. This IS was recovered from an HCC sample derived from mouse 95 that had been injected with AAV2/8.TBG.*EGFP*. It accounted for 28% of all reads and mapped to the *Rian* locus, located in the vicinity of other *Rian* integrations both previously associated with HCC and arising from vectors with TBG promoters (Figure 3).[7] We did not recover a corresponding integration on the other side of the *Rian* locus in this HCC.

As depicted in the sequence logo (Figure 4), the 150 nt of sequence surrounding the genotoxic integration in the *Rian* locus is fairly well conserved among 31 mammals. This conservation includes rodents, as well as primates, and widely encompasses the 5′ and 3′ flanking sequences of the integration event. This sequence was further inspected for homology to *AAVS1* locus (chr19:50,900,000–58,617,616) and none was detected (data not shown).

No liver tumorigenesis in MPS VI cats following long-term AAV-mediated hepatic gene transfer

MPS VI cats received, on post-natal day 50 (p50), a single systemic administration of AAV2/8.TBG vector encoding the feline ARSB (AAV2/8.TBG.*fARSB*) at the dose of 2×10^{12} GC/kg and were followed-up long term. Above or close to normal serum ARSB activity

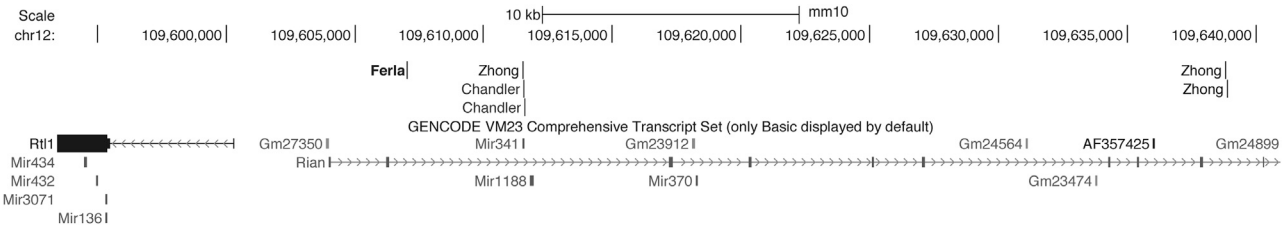

Figure 3. HCC-associated integration of AAV

Genomic locations (UCSC Genome Browser, Genome Reference Consortium Mouse Build 38 December 2012, mm10) on Chromosome 12 of rAAV HCC integrations arising only from vectors with TBG promoter.[5,6,13,20]

was detected in all cats up to the end of the study, indicating that stable liver transduction was achieved following a single vector injection (Figure 5). Liver ultrasound was performed on MPS VI cats, without evidence of masses or other liver abnormalities (Table S2). Cat #7742 was followed up to about 8.5 years of age (3,065 days) when euthanasia was required because of limb paresis that was attributed to the presence of a focal meningioma, as revealed by microscopic evaluation. Liver histopathology did not reveal any sign of malignant transformation (Figure S3). Cats #8194 and 8197 were terminated when they were about 8 years old (2,878 days old). Liver histopathology was performed on both cats. No microscopic abnormalities were observed: liver was characterized by normal lobular architecture, portal tracts were within normal limits, and hepatocytes were not vacuolated (Figure S3). Thus, data obtained in MPS VI cats, together with those generated in mice, support the low risk of tumorigenicity associated with long-term AAV-mediated gene transfer to juvenile/young adult liver using doses of vectors between 10^{12} and 10^{13} GC/kg.

DISCUSSION

In the present study, we investigated the potential tumorigenic risk associated with long-term AAV-mediated liver gene transfer in young adult mice and juvenile cats after delivery of a variety of therapeutic and reporter AAV2/8 vectors, ranging in dose between 2×10^{12} to 2×10^{13} GC/kg.

Most of the tumors found in livers were round cell neoplasms, which spontaneously arise in aging colonies[16] and are not associated with the high (>100 ng/mL) AFP levels found in mice bearing hepatic tumors. This confirms the potential utility of serum AFP as a screening marker for mouse HCC as already reported for humans (Figure S2).[18]

Our data showed that HCCs were exclusively found in AAV-treated males at an incidence (15.4%) that was not statistically different than in control mice (0%, p = 0.07; Figure 1). Spontaneous HCC formation is reported in aging colonies of C57BL/6 mice.[9,15,21] The absence of HCC in control mice may be explained by the lower number of animals in this group (n = 46) compared to the AAV-treated group (n = 76). Also, HCC were not found in female mice. We investigated if this finding could be associated to the higher AAV-mediated liver transduction in male than in female mice reported by previous studies.[22,23] No gender-related differences in terms of both GC and serum ARSB activity were observed in mice treated with 2×10^{13} GC/kg of AAV2/8 vectors (Figure 2), suggesting that this vector dose is possibly saturating and ultimately overcomes any sex-dependent difference in liver transduction. Therefore at least for this dose cohort, the different HCC incidence between males and females may be explained by the role of the androgen pathway in liver carcinogenesis,[24,25] with the exception of the HCC in which a clear correlation with AAV integration in the *Rian* locus has been found.

Conversely, both AAV GC and serum ARSB activity were higher in male than in female mice treated with AAV2/8 at the dose of 2×10^{12} GC/kg. It is therefore possible that in this group the higher HCC incidence is correlated with the higher AAV liver transduction levels observed in males than in females. On the other hand, the HCC incidence observed (1 out 10, 10%) is close to the spontaneous HCC formation rate reported in aging C57BL/6 male mice (8%–9%) and importantly no relevant AAV-ISs were identified in this HCC.[9,15]

Unlike what has been observed in mice treated as newborns,[5,6,20,26] which were typically treated with higher AAV doses than those used here, the animals treated with similarly configured cassettes did not develop HCCs at high rates.

However, the recovery of a genotoxic integration from one HCC which developed in a liver of a mouse treated with an AAV2/8.TBG.*EGFP*, deserves further commentary. While male mice receiving AAV2/8.TBG.*hARSB*-showed an overall incidence of HCC formation similar to that spontaneously observed in the aging colony of male C57BL/6 mice, i.e., about 8%–9%,[9,15] HCC incidence was 30% in mice receiving the AAV2/8.TBG.*EGFP* vector (Figure 1). Although increasing the number of animals per experimental group may increase the chance to see additional HCCs even in other experimental groups, whether the expression of EGFP, which is a non-endogenous, potentially immunogenic protein,[27] caused inflammation, and created an environment prone to tumor development remains a consideration. Indeed, the connection between inflammation and HCC development is well-known.[28,29] A previous study from Bell et al.[10] reported an increased incidence of HCC in mice treated with AAV vectors expressing the bacterial reporter LacZ compared to those receiving a therapeutic mammalian transgene. Furthermore, later studies on an HCC from a mouse treated with the AAV bearing

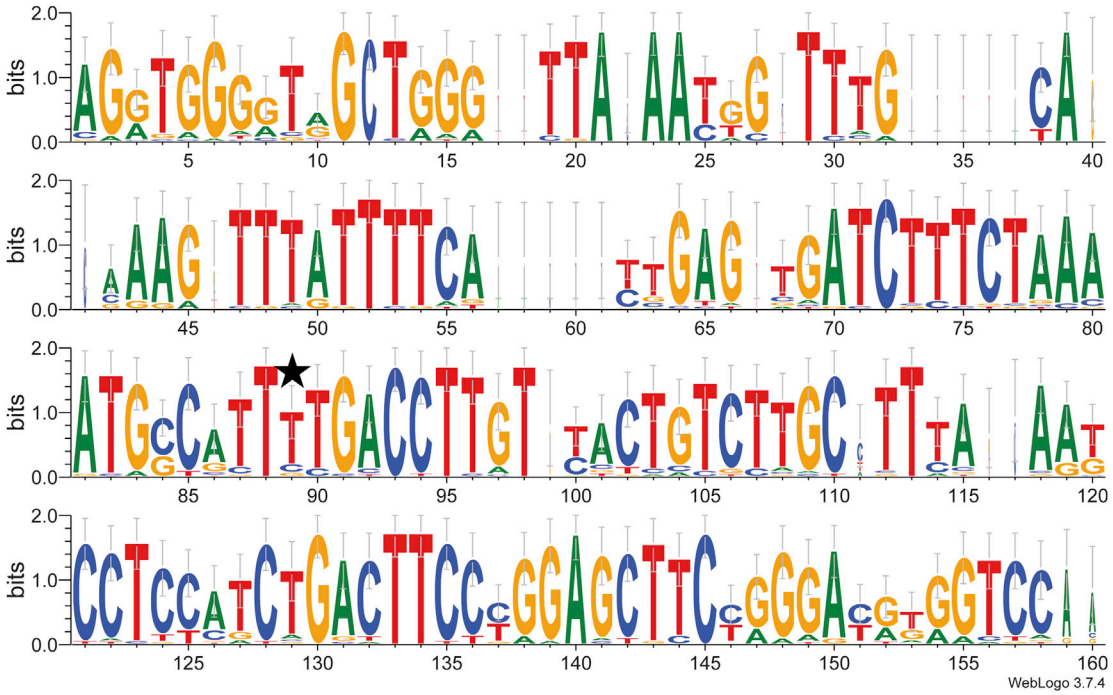

Figure 4. Genomic conservation around the integration site in the mouse *Rian* locus

The asterisk indicates the position of the integration site. This logo is a graphical representation of a multiple sequence alignment of genomic DNA derived from 31 mammals. The height of each letter indicates its frequency at that position. The overall height of the stack of letters depicts the information content (measured in bits) and reflects the sequence conservation at that position.

the therapeutic gene in this same study was found to harbor a genotoxic integration in *Rian* (Figure 3).[13] For this reason, genomic analyses were conducted, and our results explain the formation of at least one AAV HCC in the AAV2/8.TBG.*EGFP*-treated mice.

Our results are consistent with previous studies showing no increased risk of tumor formation in large cohorts of adult mice receiving a variety of different AAV vectors for liver-directed gene transfer.[9–11] However, the value of those previous studies,[9] endorsing the low tumorigenesis risk associated with AAV-mediated liver gene transfer was limited by the short follow-up compared to the other studies in newborn mice, which indeed showed that in most cases HCC arose between 14 and 25 months of age.[5,6] Also, where a long-term follow-up was performed,[11] data were restricted to the combination of a self-complementary AAV with the liver-specific promoter 1 (LP1), which both showed no safety concerns in newborn rats and mice, respectively.[5,30] Therefore, our study addresses with a 2-year prospective follow-up, the risk of tumorigenicity in joung adult mice that received single-stranded, hepatotrophic AAVs containing different liver-specific promoters and different transgenes. Our data suggest that the risk is low, although the doses used here are considerably lower than other studies that observed HCC in mice after neonatal AAV gene therapy. Neonatal gene transfer with traditional AAVs indeed relies on high dose of vectors (in the order of 10^{14} GC/kg or higher) to counteract the dilution of episomal AAV DNA due to the hepatocyte proliferation.[5,6,20,26] Conversely, our doses are similar to those (ranging from 2×10^{12} to 4×10^{13} GC/kg) used when adult mice were treated with AAV to assess genotoxicity.[9,10,12] To the best of our knowledge, only Li et al.[11] tested up to 1×10^{14} GC/kg in adult mice.

Doses spanning in the range of 10^{14} GC/kg have been used in recent clinical trials (e.g., NCT03199469, X-linked myotubular myopathy), as well as for the approved Zolgensma, both targeting a very young population (infant-toddler). However, other gene therapy clinical trials use doses, which are in the range (10^{12}–10^{13} GC/kg) tested in our study (NTC02991144, NTC04088734, NCT03001830, NCT02576795, NCT01620801), making our findings relevant and comforting in the field of gene therapy, further confirming that toxicity appears dose dependent.

Specifically, for the MPS VI clinical trial (NTC03173521), therapeutic doses have been widely investigated and validated in a pre-clinical setting in both feline and murine models of MPS VI.[14,31–33] The vector doses at which we have observed a therapeutic effect ranged between 2×10^{11} and 2×10^{12} GC/kg. Therefore, the doses we tested in the current study, i.e., either 2×10^{12} or 2×10^{13} GC/kg, are in or well beyond (1 log), respectively, the range of therapeutically relevant doses defined in preclinical studies and translated to the clinic.

In addition, we show there are no liver cancers in the three MPS cats followed up to 8 years following vector administration. Future efforts

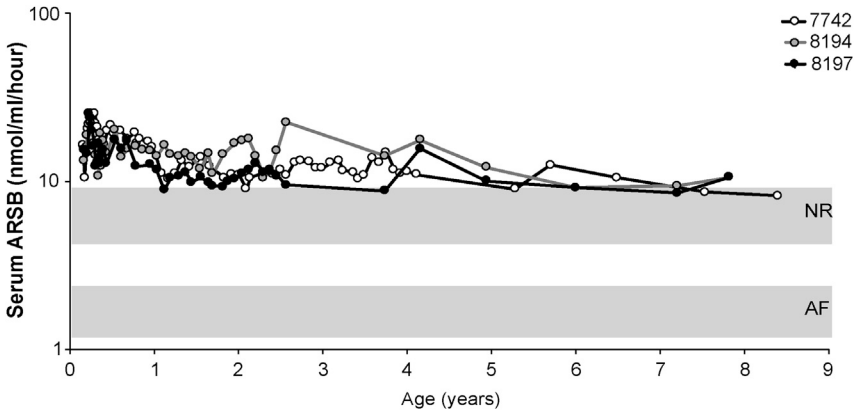

Figure 5. Serum ARSB activity in MPS VI cats treated with AAV2/8.TBG.*fARSB*

MPS VI cats were injected at postnatal days 50 with 2×10^{12} GC/kg of AAV2/8.TBG.*fARSB*. Serum ARSB activity was monitored over time after vector administration. Each line represents ARSB values over time from a single animal. The upper and lower gray areas represent the range of serum ARSB activity values in normal (NR) and affected (AF) cats, respectively. AAV2/8, adeno-associated viral vectors serotype 8; TBG, thyroxine-binding globulin; *fARSB*, feline arylsulfatase B.

will focus on the development of an integration pipeline for the feline genome, with the subsequent capture and analysis of AAV integrations in the treated MPS VI cats as was done for the murine models. Although the low number of MPS VI cats makes the study purely observational, the data collected are consistent with other long-term studies in large animal models, such as dogs[34] and non-human primates (NHPs),[35,36] in which tumorigenicity associated with AAV hepatic gene transfer has not yet been observed. Also, serum ARSB levels in MPS VI cats were stable over time (Figure 5), suggesting that if integration had occurred, it was not associated with subsequent *in vivo* expansion.

The pattern of integrations we have observed after systemic AAV gene delivery with AAV2/8.TBG vectors in mice is worthy of commentary. As others have previously documented,[10,11,13] the relative numbers of AAV integrations recovered in young adult mice after treatment with AAV is rather low, with only several hundred integrations recovered per mouse (Table S1). We took an additional measure in the pre-analysis step to mitigate any possible artifacts that could be derived from the pipeline, sample processing, and/or tissue contamination and removed any site that had the same coordinate as an IS recovered from any study we have conducted over the past 5 years (n = 5). Such filtering is conservative, as there is evidence for identical ISs being recovered by independent labs using different AAV vectors and different pipelines for the identification of integrations but affords more confidence in our final list of ISs (Table S1). In the future, a combination of tiling with LAM-PCR amplification and long read NGS may be needed to characterize AAV integrations to ensure that both sides of the event are captured for genomic analyses.

To further narrow our focus, we restricted our analysis to events that had relatively high read counts (>5,000), and then further, on only those seen in HCCs compared to controls, reasoning that those integrations may be causative under a model of insertional activation. After this analysis, only one locus emerged as a likely genotoxic integration. Mouse 95 had a single integration event that was confirmed after amplification with independent bar codes, and mapped very close to *Mir341*, within the *Rian* locus. In complete agreement with previous studies that have used AAV8.TBG vectors in mouse models of OTC deficiency and methylmalonic acidemia (MMA) and observed HCC formation afterward,[5,13] the event we captured has only a single ITR detected, and is located very close to the *Rtl1* gene (Figure 3), the suspected driver of HCC formation after AAV integration in mice.[37] It should be noted that we were successful in recovering what we interpret as a clonal and pathogenic integration in only 1 of 6 HCCs. Whether the other HCCs we found in the course of our study were driven by AAV, or coincidental, remains unknown but highlights the need for future studies to include genome sequencing in the integration analysis pipeline, especially since the genotoxic event we recovered maps outside of the *Mir341* gene, and in a region of the mouse genome that is widely conserved between mice and humans (Figure 4).

While the identification of at least one event that clearly suggests AAV-mediated genotoxicity has safety and monitoring ramifications, it should be noted that AAV integration has not yet been associated with hepatic genotoxicity in NHPs or noted in hemophilia B subjects as long as 10 years post-gene transfer,[38] or in any of a dozen clinical trials based on AAVs, although an extended follow-up is certainly required.

In conclusion, our study suggests that exposure of the juvenile/young adult liver to doses of AAV up to 2×10^{13} GC/kg, approximating what will be used in many clinical applications, carries a low tumorigenesis risk, likely because hepatocyte proliferation is reduced, which should enable long-term transgene expression by avoiding/minimizing the loss of episomal AAV genomes.

However, results from the integration analysis performed in our study suggest that clonal and pathogenic integrations may still occur and must be taken into consideration when monitoring subjects involved in clinical trials based on AAV-mediated liver gene transfer.

MATERIALS AND METHODS

Animal colonies

C57BL/6 mice were maintained at the IGB Animal House Facility (Naples, Italy). Animals were raised in accordance with the

Institutional Animal Care and Use Committee (IACUC) guidelines for the care and use of animals in research. After treatment, health status was recorded twice a day, in the morning and at the end of the working day. Abdominal palpation to check for eventual hepatic tumors formation was performed from 9 months post-injection on a monthly schedule and from 21 months post-injection on a weekly schedule (Figure S1).

The feline model of MPS VI colony was maintained at the University of Pennsylvania, School of Veterinary Medicine. Animals were raised under National Institutes of Health (NIH) and U.S. Department of Agriculture (USDA) guidelines and in accordance with the Institutional Animal Care and Use Committee (IACUC) guideline for the care and use of animals in research. The genotype was determined by polymerase chain reaction (PCR). Daily observations were performed on treated MPS VI cats. All experiments performed in animals are conform to the relevant regulatory standards.

Vector production

The following AAV2/8 vectors were used in this study: AAV2/8 vectors encoding *hARSB*-, the *fARSB*, and the *EGFP* under the control of the liver specific TBG promoter and the alpha-1-microglobulin/bikunin precursor. i.e., AAV2/8.TBG.*hARSB*, AAV2/8.TBG.*fARSB*, and AAV2/8.TBG.*EGFP*, respectively, and the vector encoding the *hARSB* under the control of the LP1, i.e., AAV2/8.LP1.*hARSB*.[39] All vectors were produced by the AAV Vector Core of Telethon Institute of Genetics and Medicine (TIGEM) (Pozzuoli, Italy), as previously described.[40]

Vector Administration

Young adult (6–8 weeks old) C57BL/6 mice from Harlan Laboratories were injected in the retro-orbital sinus. 20 mice per test group, i.e., 10 males (M) and 10 females (F), were treated as follows (Table 1): 2×10^{13} GC/kg of AAV2/8.TBG.*hARSB* (TEST 1), 2×10^{12} GC/kg of AAV2/8.TBG.*hARSB* (TEST 2), 2×10^{13} GC/kg of AAV2/8.LP1.*hARSB* (TEST 3), and 2×10^{13} GC/kg of AAV2/8.TBG.*EGFP* (TEST 4). As control, mice were (1) left untreated (CTR 1, 10M+10F); (2) treated with the excipient 1 (CTR 2, 10M+10F), which was PBS 5% glycerol diluted 1:1.5 in NaCl 0.9% saline solution to mimic the final formulation of vectors administered in TEST 1, 3, and 4; or (3) treated with the excipient 2 (CTR3, 5M+5F), which was PBS 5% glycerol diluted 1:15 in NaCl 0.9% saline solution to mimic the final formulation of vectors administered in TEST 2 (Table 1).

MPS VI cats were injected at postal natal day 50 (p50) with 2×10^{12} GC/kg of AAV2/8.TBG.*fARSB* vector delivered through a catheter placed in the cephalic vein.

Blood and tissue collection

Blood was collected from the retro-orbital sinus of mice on months 12, 18, and 21 post-injection and at sacrifice (Figure S1). In MPS VI cats, blood collection was performed from the cephalic vein using a 22G needle at several time-points following AAV vector administration. Blood was centrifuged at 10,000 × *g* in a microcentrifuge for 10 min at 4°C to obtain the serum. Mice were terminated at 24 months post-injection, unless euthanasia was required because of bad health conditions or an evident abdominal mass. Cats were terminated at about 8–8.5 years of age. Liver (all four main lobes) and any organ/tissue showing abnormalities were collected following cardiac perfusion with PBS, except in mice found dead in which organs harvesting was performed wherever possible. When a mass was identified at necropsy, a sample of normal tissue adjacent to the mass was harvested unless the whole organ was interested. Organs were immediately frozen in dry ice for either DNA integration analysis or AAV quantification or fixed for histopathology.

Histopathology

Tissues no more than 0.5 cm thick were fixed by immersion in Formalin Solution, Neutral buffered 10% (Sigma Aldrich, St. Louis, MO, USA) for at least 3 days and then put in 70% ethanol (Sigma Aldrich, St. Louis, MO, USA). Fixed samples were processed routinely, embedded in paraffin, and sectioned at 4 μm thickness. Sections were then stained with hematoxylin and eosin (H&E) using standard methods. All samples were reviewed by a board-certified veterinary pathologist. Findings were classified using the (International Harmonization of Nomenclature and Diagnostic Criteria (INHAND) monograph.[41] All sections were examined using a BX11 microscope (Olympus, Tokyo, Japan).

Liver ultrasound

Liver ultrasound was performed by manually restraining the cat in dorsal recumbancy while the single organ scan is performed and interpreted by a board-certified radiologist. Scans were done on a GE Medical 9L machine using a 2.7–7.8 MHz linear transducer (GE Healthcare, Chicago, IL, USA).

Integration analysis

DNA was obtained from tumor and matched control tissues using the DNeasy Tissue and Blood Kit (QIAGEN, Hilden, Germany), following the manufacturer's instructions. Integration site recovery was performed as previously described.[5,42] Briefly, DNA was digested independently with restriction enzymes MspI and Csp61. The independent digests for each sample were then pooled and barcoded. Following a nested PCR using primers specific to the barcoded linkers and AAV ITR-specific primers, the samples were then sequenced using the Illumina MiSeq platform. Unique ISs were deconvoluted after sequencing using the Genomic Integration Site Tracker pipeline (GeIST, https://github.com/mlafave/GeIST)[5,19] and mapped to the mouse reference genome, with an additional step that discarded all reads that mapped to the vectors. The final step was to ensure that the resulting ISs were of high quality and did not result from any artifacts of our experimental or computational pipeline. We compared the recovered IS to the 26,498 unique IS that we have amassed from 5 independent analyses of mouse AAV ISs using the GeIST pipeline, and removed from this dataset any IS that we had detected previously (Wolfsberg et al., unpublished data).[5] However, because

other studies have identified and validated IS in the *Rian* locus and/or delineated, in different studies, exactly the same ISs in the *Alb* gene,[11] we retained all ISs near those loci, even if they were seen in any of the other five datasets.

Comparative genomic analysis of the AAV8.TBG.*EGFP Rian* integration

The conserved genomic sequences around the integration site in the mouse *Rian* locus (chr12:109607025 on GRCm38/mm10) were derived from the Conservation: Multiz Alignments of 60 Vertebrates track on the UCSC Genome Browser. We selected the region of this track that covered mouse chr12:109606956–109607087, and extracted the corresponding aligned sequences from the following 31 mammalian genomes: mouse, human, baboon, bush baby, cat, chimp, cow, dog, dolphin, elephant, gibbon, gorilla, guinea pig, horse, kangaroo rat, manatee, marmoset, megabat, microbat, mouse lemur, naked mole rat, orangutan, panda, rabbit, rat, rhesus, sheep, squirrel, squirrel monkey, tarsier, and tree shrew. For the gorilla genome, we substituted the sequence from genome assembly GorGor5, rather than the GorGor3 assembly used by Multiz. Genome sequences were re-aligned using the MUSCLE sequence alignment tool (version 3.8, default parameters) at https://www.ebi.ac.uk/Tools/msa/muscle/. We then created a sequence logo of this alignment using the default parameters of WebLogo at http://weblogo.threeplusone.com/.

ARSB activity and alpha-fetoprotein levels measurement

Serum ARSB activity was measured by an immune capture assay based on the use of a specific custom-made anti-hARSB polyclonal antibody (Covalab, Villeurbanne, France), as previously described.[32] As control, endogenous (murine) serum ARSB activity was measured in C57BL/6 males and females that not received AAV2/8.*hARSB* vectors, which include mice untreated or injected with the excipient (n = 5/sex) and mice receiving 2×10^{13} GC/kg of AAV2/8.TBG.*EGFP* (n = 6/sex). The mean value measured in controls was subtracted to the value measure in each AAV2/8.*hARSB*-treated mouse to obtain a measure of hARSB activity deriving from AAV2/8 vectors. AFP levels were determined in serum from mice using the mouse Alfa-Fetoprotein/AFP Quantikine Elisa Kit (R&D Systems, Minneapolis, MN, USA), following the manufacturer's instructions.

Quantification of AAV DNA in liver

Genomic DNA was extracted from livers using a DNeasy Blood and Tissue Extraction kit (QIAGEN, Hilden, Germany), following the manufacturer's instructions. Real-time qPCR analysis was performed on 100 ng of total DNA using a set of primers/probe specific for the bovine growth hormone (BGH) poly(A) in the viral genome and TaqMan universal PCR master mix (Applied Biosystems, Foster City, CA), as previously described.[33] Amplification was run on LightCycler 96 (Roche, Mannheim, Germany) with standard cycles. All the reactions were performed in triplicate.

Statistical analysis

The Fisher's exact test was used to evaluate the incidence of HCCs (Figure 1) and other tumors found in livers and to assess whether AFP levels >100 ng/mL were predictive of hepatic pathology. All statistical computings were made by using the function fisher.test () of stats package of R software (R version 3.6.1).

AFP levels over time (Figure S1) are expressed as mean ± standard error (SE). A two-way ANOVA followed by the Tukey post hoc test was conducted to examine the effects of "group" and "time" on AFP score. There was a statistically significant interaction between "group" and "time" on AFP score (p = 3.44e-11 and eta-squared or effect size n2g = 0.2). Bonferroni adjustment was applied.

AAV liver DNA and serum ARSB activity (Figure 2) are expressed as mean ± SE. The Kruskal-Wallis test followed by the Dunn's test was conducted to perform multiple pairwise comparisons between experimental groups. The Kruskal-Wallis p value is <0.001. Bonferroni adjustment was applied. The Wilcoxon rank sum test was used for direct comparisons between males and females for each group of treatment. All statistical computing was made by using rstatix package of R software (R version 3.6.1).

Statistical p values <0.05 were considered significant. More details about statistical analyses are reported in the Supplemental Methods results section.

A prospective power analysis based on Fisher's exact test was performed for sample size estimation, using the G * Power 3.1. software. We used data available for spontaneous HCC incidence and AAV-related HCC incidence.[5,15] The minimum sample size ranged between 8 and 11 animals for each treatment group, using a significance level $\alpha = 0.05$, a power $(1- \beta) = 0.80$ and event rates p1 and p2 equal to 8% and 82% for control and AAV-treated males, respectively, and 7% and 69% for control and AAV-treated females, respectively.

SUPPLEMENTAL INFORMATION

Supplemental Information can be found online at https://doi.org/10.1016/j.omtm.2020.11.015.

ACKNOWLEDGMENTS

This research was supported by the European Commission Seventh Framework Programme(FP7/2007–2013) (MeuSIX grant 304999), European Union Horizon 2020(Upgrade grant 825825), the Isaac Foundation and in part by the Intramural Research Program of the National Human Genome Research Institute at the National Institutes of Health (grant number 1ZIAHG200318-16), United States. We gratefully acknowledge Antonella Iuliano (TIGEM Bioinformatics Core) for statistical analyses, the TIGEM AAV vector core for vector production, and the staff of the NIH Intramural Sequencing Center for sequencing the regions around the integration sites.

AUTHOR CONTRIBUTIONS

R.F. and A.A. conceived the study; A.-D.N. and Z.C. were involved in programming and software development; T.G.W. validated data; R.F., M.A., M.D., E.N., J.C., S.N.S., P.O., P.W., and C.V. conducted experiments, performed the investigation process, and collected data; J.C.,

T.G.W., A.-D.N., Z.C., M.H., C.V., and C.P.V. provided resources; T.G.W., A.-D.N., and Z.C. worked on data curation; R.F., S.N.S., T.G.W., and A.-D.N. worked on visualization and data presentation; R.F., C.V.P., and A.A. wrote the original draft; R.F., J.C., S.N.S., T.G.W., R.J.C., S.M.B., C.V., M.H., C.P.V., and A.A. contributed to writing, reviewing, and editing the manuscript; R.F., C.P.V., S.M.B., and A.A oversaw the planning and execution of research activities; S.M.B., C.P.V., and A.A acquired financial support.

DECLARATION OF INTERESTS

A.A. is founder and consultant of InnovaVector srl. The other authors have no competing interests to declare.

REFERENCES

1. Brunetti-Pierri, N., and Auricchio, A. (2010). Gene Therapy of Human Inherited Diseases. In The Metabolic and Molecular Bases of Inherited Diseases, R. Scriver, ed. (New York: McGraw Hill), pp. 1–50.
2. Weitzman, M.D., and Linden, R.M. (2011). Adeno-Associated Virus Biology. In Adeno-Associated Virus Methods and Protocols, R.O. Snyder and P. Moullier, eds. (Humana Press), pp. 1–16.
3. Balakrishnan, B., and Jayandharan, G.R. (2014). Basic biology of adeno-associated virus (AAV) vectors used in gene therapy. Curr. Gene Ther. *14*, 86–100.
4. Colella, P., Ronzitti, G., and Mingozzi, F. (2017). Emerging Issues in AAV-Mediated *In Vivo* Gene Therapy. Mol. Ther. Methods Clin. Dev. *8*, 87–104.
5. Chandler, R.J., LaFave, M.C., Varshney, G.K., Trivedi, N.S., Carrillo-Carrasco, N., Senac, J.S., Wu, W., Hoffmann, V., Elkahloun, A.G., Burgess, S.M., and Venditti, C.P. (2015). Vector design influences hepatic genotoxicity after adeno-associated virus gene therapy. J. Clin. Invest. *125*, 870–880.
6. Donsante, A., Miller, D.G., Li, Y., Vogler, C., Brunt, E.M., Russell, D.W., and Sands, M.S. (2007). AAV vector integration sites in mouse hepatocellular carcinoma. Science *317*, 477.
7. Chandler, R.J., Sands, M.S., and Venditti, C.P. (2017). Recombinant Adeno-Associated Viral Integration and Genotoxicity: Insights from Animal Models. Hum. Gene Ther. *28*, 314–322.
8. Luk, J.M., Burchard, J., Zhang, C., Liu, A.M., Wong, K.F., Shek, F.H., Lee, N.P., Fan, S.T., Poon, R.T., Ivanovska, I., et al. (2011). DLK1-DIO3 genomic imprinted microRNA cluster at 14q32.2 defines a stemlike subtype of hepatocellular carcinoma associated with poor survival. J. Biol. Chem. *286*, 30706–30713.
9. Bell, P., Wang, L., Lebherz, C., Flieder, D.B., Bove, M.S., Wu, D., Gao, G.P., Wilson, J.M., and Wivel, N.A. (2005). No evidence for tumorigenesis of AAV vectors in a large-scale study in mice. Mol. Ther. *12*, 299–306.
10. Bell, P., Moscioni, A.D., McCarter, R.J., Wu, D., Gao, G., Hoang, A., Sanmiguel, J.C., Sun, X., Wivel, N.A., Raper, S.E., et al. (2006). Analysis of tumors arising in male B6C3F1 mice with and without AAV vector delivery to liver. Mol. Ther. *14*, 34–44.
11. Li, H., Malani, N., Hamilton, S.R., Schlachterman, A., Bussadori, G., Edmonson, S.E., Shah, R., Arruda, V.R., Mingozzi, F., Wright, J.F., et al. (2011). Assessing the potential for AAV vector genotoxicity in a murine model. Blood *117*, 3311–3319.
12. Rosas, L.E., Grieves, J.L., Zaraspe, K., La Perle, K.M., Fu, H., and McCarty, D.M. (2012). Patterns of scAAV vector insertion associated with oncogenic events in a mouse model for genotoxicity. Mol. Ther. *20*, 2098–2110.
13. Zhong, L., Malani, N., Li, M., Brady, T., Xie, J., Bell, P., Li, S., Jones, H., Wilson, J.M., Flotte, T.R., et al. (2013). Recombinant adeno-associated virus integration sites in murine liver after ornithine transcarbamylase gene correction. Hum. Gene Ther. *24*, 520–525.
14. Cotugno, G., Annunziata, P., Tessitore, A., O'Malley, T., Capalbo, A., Faella, A., Bartolomeo, R., O'Donnell, P., Wang, P., Russo, F., et al. (2011). Long-term amelioration of feline Mucopolysaccharidosis VI after AAV-mediated liver gene transfer. Mol. Ther. *19*, 461–469.
15. Frith, C.H., and Wiley, L. (1982). Spontaneous hepatocellular neoplasms and hepatic hemangiosarcomas in several strains of mice. Lab. Anim. Sci. *32*, 157–162.
16. Brayton, C. (2007). Spontaneous Diseases in Commonly Used Mouse Strains. In The Mouse in Biomedical Research (Elsevier), pp. 623–717.
17. Becker, F.F., Stillman, D., and Sell, S. (1977). Serum alpha-fetoprotein in a mouse strain (C3H-Avy fB) with spontaneous hepatocellular carcinomas. Cancer Res. *37*, 870–872.
18. Yamashita, T., Forgues, M., Wang, W., Kim, J.W., Ye, Q., Jia, H., Budhu, A., Zanetti, K.A., Chen, Y., Qin, L.X., et al. (2008). EpCAM and alpha-fetoprotein expression defines novel prognostic subtypes of hepatocellular carcinoma. Cancer Res. *68*, 1451–1461.
19. LaFave, M.C., Varshney, G.K., and Burgess, S.M. (2015). GeIST: a pipeline for mapping integrated DNA elements. Bioinformatics *31*, 3219–3221.
20. Walia, J.S., Altaleb, N., Bello, A., Kruck, C., LaFave, M.C., Varshney, G.K., Burgess, S.M., Chowdhury, B., Hurlbut, D., Hemming, R., et al. (2015). Long-term correction of Sandhoff disease following intravenous delivery of rAAV9 to mouse neonates. Mol. Ther. *23*, 414–422.
21. Blackwell, B.N., Bucci, T.J., Hart, R.W., and Turturro, A. (1995). Longevity, body weight, and neoplasia in ad libitum-fed and diet-restricted C57BL6 mice fed NIH-31 open formula diet. Toxicol. Pathol. *23*, 570–582.
22. Davidoff, A.M., Ng, C.Y., Zhou, J., Spence, Y., and Nathwani, A.C. (2003). Sex significantly influences transduction of murine liver by recombinant adeno-associated viral vectors through an androgen-dependent pathway. Blood *102*, 480–488.
23. Pañeda, A., Vanrell, L., Mauleon, I., Crettaz, J.S., Berraondo, P., Timmermans, E.J., Beattie, S.G., Twisk, J., van Deventer, S., Prieto, J., et al. (2009). Effect of adeno-associated virus serotype and genomic structure on liver transduction and biodistribution in mice of both genders. Hum. Gene Ther. *20*, 908–917.
24. Drinkwater, N.R., Hanigan, M.H., and Kemp, C.J. (1990). Genetic and epigenetic promotion of murine hepatocarcinogenesis. Prog. Clin. Biol. Res. *331*, 163–176.
25. Kemp, C.J., and Drinkwater, N.R. (1990). The androgen receptor and liver tumor development in mice. Prog. Clin. Biol. Res. *331*, 203–214.
26. Donsante, A., Vogler, C., Muzyczka, N., Crawford, J.M., Barker, J., Flotte, T., Campbell-Thompson, M., Daly, T., and Sands, M.S. (2001). Observed incidence of tumorigenesis in long-term rodent studies of rAAV vectors. Gene Ther. *8*, 1343–1346.
27. Ansari, A.M., Ahmed, A.K., Matsangos, A.E., Lay, F., Born, L.J., Marti, G., Harmon, J.W., and Sun, Z. (2016). Cellular GFP Toxicity and Immunogenicity: Potential Confounders in in Vivo Cell Tracking Experiments. Stem Cell Rev. Rep. *12*, 553–559.
28. Berasain, C., Castillo, J., Perugorria, M.J., Latasa, M.U., Prieto, J., and Avila, M.A. (2009). Inflammation and liver cancer: new molecular links. Ann. N Y Acad. Sci. *1155*, 206–221.
29. Yang, Y.M., Kim, S.Y., and Seki, E. (2019). Inflammation and Liver Cancer: Molecular Mechanisms and Therapeutic Targets. Semin. Liver Dis. *39*, 26–42.
30. Gauttier, V., Pichard, V., Aubert, D., Kaeppel, C., Schmidt, M., Ferry, N., and Conchon, S. (2013). No tumour-initiating risk associated with scAAV transduction in newborn rat liver. Gene Ther. *20*, 779–784.
31. Ferla, R., O'Malley, T., Calcedo, R., O'Donnell, P., Wang, P., Cotugno, G., Claudiani, P., Wilson, J.M., Haskins, M., and Auricchio, A. (2013). Gene therapy for mucopolysaccharidosis type VI is effective in cats without pre-existing immunity to AAV8. Hum. Gene Ther. *24*, 163–169.
32. Ferla, R., Claudiani, P., Cotugno, G., Saccone, P., De Leonibus, E., and Auricchio, A. (2014). Similar therapeutic efficacy between a single administration of gene therapy and multiple administrations of recombinant enzyme in a mouse model of lysosomal storage disease. Hum. Gene Ther. *25*, 609–618.
33. Ferla, R., Alliegro, M., Marteau, J.B., Dell'Anno, M., Nusco, E., Pouillot, S., Galimberti, S., Valsecchi, M.G., Zuliani, V., and Auricchio, A. (2017). Non-clinical Safety and Efficacy of an AAV2/8 Vector Administered Intravenously for Treatment of Mucopolysaccharidosis Type VI. Mol. Ther. Methods Clin. Dev. *6*, 143–158.
34. Niemeyer, G.P., Herzog, R.W., Mount, J., Arruda, V.R., Tillson, D.M., Hathcock, J., van Ginkel, F.W., High, K.A., and Lothrop, C.D., Jr. (2009). Long-term correction of inhibitor-prone hemophilia B dogs treated with liver-directed AAV2-mediated factor IX gene therapy. Blood *113*, 797–806.

35. Gil-Farina, I., Fronza, R., Kaeppel, C., Lopez-Franco, E., Ferreira, V., D'Avola, D., Benito, A., Prieto, J., Petry, H., Gonzalez-Aseguinolaza, G., and Schmidt, M. (2016). Recombinant AAV Integration Is Not Associated With Hepatic Genotoxicity in Nonhuman Primates and Patients. Mol. Ther. *24*, 1100–1105.

36. Nathwani, A.C., Rosales, C., McIntosh, J., Rastegarlari, G., Nathwani, D., Raj, D., Nawathe, S., Waddington, S.N., Bronson, R., Jackson, S., et al. (2011). Long-term safety and efficacy following systemic administration of a self-complementary AAV vector encoding human FIX pseudotyped with serotype 5 and 8 capsid proteins. Mol. Ther. *19*, 876–885.

37. Wang, P.R., Xu, M., Toffanin, S., Li, Y., Llovet, J.M., and Russell, D.W. (2012). Induction of hepatocellular carcinoma by in vivo gene targeting. Proc. Natl. Acad. Sci. USA *109*, 11264–11269.

38. Nathwani, A.C., Reiss, U.M., Tuddenham, E.G., Rosales, C., Chowdary, P., McIntosh, J., Della Peruta, M., Lheriteau, E., Patel, N., Raj, D., et al. (2014). Long-term safety and efficacy of factor IX gene therapy in hemophilia B. N. Engl. J. Med. *371*, 1994–2004.

39. Nathwani, A.C., Gray, J.T., Ng, C.Y., Zhou, J., Spence, Y., Waddington, S.N., Tuddenham, E.G., Kemball-Cook, G., McIntosh, J., Boon-Spijker, M., et al. (2006). Self-complementary adeno-associated virus vectors containing a novel liver-specific human factor IX expression cassette enable highly efficient transduction of murine and nonhuman primate liver. Blood *107*, 2653–2661.

40. Tessitore, A., Faella, A., O'Malley, T., Cotugno, G., Doria, M., Kunieda, T., Matarese, G., Haskins, M., and Auricchio, A. (2008). Biochemical, pathological, and skeletal improvement of mucopolysaccharidosis VI after gene transfer to liver but not to muscle. Mol. Ther. *16*, 30–37.

41. Thoolen, B., Maronpot, R.R., Harada, T., Nyska, A., Rousseaux, C., Nolte, T., Malarkey, D.E., Kaufmann, W., Küttler, K., Deschl, U., et al. (2010). Proliferative and nonproliferative lesions of the rat and mouse hepatobiliary system. Toxicol. Pathol. *38* (7, Suppl), 5S–81S.

42. Chandler, R.J., LaFave, M.C., Varshney, G.K., Burgess, S.M., and Venditti, C.P. (2016). Genotoxicity in mice following AAV gene delivery: A safety concern for human gene therapy? Mol. Ther. *24*, 198–201.